Atomic Layer Deposition of SiO_2 Films on BN Particles Using Sequential Surface Reactions

J. D. Ferguson,[†] A. W. Weimer,[‡] and S. M. George*,[†]

Department of Chemistry and Biochemistry, and Department of Chemical Engineering, University of Colorado, Boulder, Colorado 80309

Received April 16, 2000. Revised Manuscript Received September 6, 2000

Alternating $SiCl_4$ and H_2O exposures were used to deposit SiO_2 films with atomic layer control on BN particles. The high surface area of the BN particles facilitated the use of transmission Fourier transform infrared (FTIR) spectroscopy to monitor the sequential surface reactions. The BN particles initially displayed vibrational modes consistent with BOH* and BNH_2* surface species. $SiCl_4$ exposure at 700 K converted these species to $SiCl_x$* surface species. The subsequent H_2O exposure at 700 K converted the $SiCl_x$* species to SiOH* surface species. Alternate exposures of $SiCl_4$ and H_2O yielded $SiCl_x$* and SiOH* species, respectively, sequentially depositing silicon and oxygen with atomic layer control. By repeating the sequential surface reactions, the absorbance of SiO_2 bulk vibrational modes on the BN particles increased versus the number of $SiCl_4$ and H_2O reaction cycles. Transmission electron microscopy studies revealed fairly uniform SiO_2 films of ∼28−38 Å on the edge planes of the BN particles after 32 reaction cycles at 700 K. SiO_2 films on the basal planes of the BN particles were thinner and occurred in patches. X-ray photoelectron spectroscopy analysis was consistent with some uncoated regions on the BN particles. These ultrathin SiO_2 films on BN particles may be useful to enhance the loading of BN particles in composite materials.

I. Introduction

Boron nitride (BN) has a very high thermal conductivity of ∼400 W/mK at 300 K.[1] This high thermal conductivity makes the addition of BN particles in composite materials desirable for thermal management applications.[2−4] However, the loading of BN particles in composites is limited by the inertness of the BN surface.[5,6] Ultrathin films can alter the chemical nature of the BN surface without adversely affecting the thermal conductivity of the BN particles. SiO_2 is a particularly attractive coating material because coupling agents have been developed for SiO_2 particles and the epoxy matrix of composite materials.[7] The SiO_2 film should be thin to minimize the effect of the oxide coating on the thermal conductivity of the BN particles.

Wet chemical processing and chemical vapor deposition techniques cannot easily control the deposition of ultrathin films on particles.[8] Uneven coatings often result because of limited conductance through convoluted pathways in particle beds.[9] Chemical vapor deposition can also cause particle agglomeration unless the particle bed is effectively agitated or fluidized.[10] In contrast, atomic layer deposition (ALD) is an ideal technique for depositing ultrathin films with precise thickness control and high conformality. Techniques have been developed for the deposition of SiO_2 using sequential surface reactions.[11−15] The virtue of this approach is that self-limiting surface reactions control the deposition at the atomic level.[16] Consequently, uniform and conformal deposition will occur on high aspect ratio porous structures[17] or particle beds.

Recent studies of SiO_2 ALD have demonstrated the growth of ultrathin films using sequential surface reactions.[12−15] This approach is based on a chemical vapor deposition (CVD) reaction for SiO_2:[18]

$$SiCl_4 + 2\ H_2O \rightarrow SiO_2 + 4\ HCl \qquad (1)$$

SiO_2 ALD is achieved by dividing this binary reaction

[†] Department of Chemistry and Biochemistry.
[‡] Department of Chemical Engineering.

(1) Sichel, E. K.; Miller, R. E.; Abrahams, M. S.; Buiocchi, C. J. *Phys. Rev. B* **1976**, *13*, 4607.
(2) Bujard, P. *Helv. Phys. Acta* **1988**, *61*, 131.
(3) Ishida, H.; Rimdusit, S. *Thermochim Acta* **1998**, *320*, 177.
(4) Wong, C. P.; Bollampally, R. S. *IEEE Trans. Adv. Pack.* **1999**, *22*, 54.
(5) Arya, S. P. S.; D'Amico, A. *Thin Solid Films* **1988**, *157*, 267.
(6) Shetty, R.; Wilcox, W. R. *J. Cryst. Growth* **1995**, *153*, 97.
(7) Gun'ko, V. M.; Voronin, E. F.; Zarko, V. I.; Pakhlov, E. M. *J. Adhes. Sci. Technol.* **1997**, *11*, 627.
(8) Dan, J. P.; Boving, H. J.; Hintermann, H. E. *J. Phys. IV* **1993**, *3*, 933.
(9) Kindl, B.; Teng, Y. H.; Liu, Y. L. *Composites* **1994**, *25*, 671.
(10) Nienow, A. W.; Rowe, P. N. Particle Growth and Coating in Gas-Fluidized Beds. In *Fluidization*; Davidson, J. F., Clift, R., Harrison, D., Eds.; Academic Press: London, 1985; p 563.
(11) Sneh, O.; Wise, M. L.; Ott, A. W.; Okada, L. A.; George, S. M. *Surf. Sci.* **1995**, *334*, 135.
(12) Klaus, J. W.; Ott, A. W.; Johnson, J. M.; George, S. M. *Appl. Phys. Lett.* **1997**, *70*, 1092.
(13) Klaus, J. W.; Sneh, O.; George, S. M. *Science* **1997**, *278*, 1934.
(14) Klaus, J. W.; Sneh, O.; Ott, A. W.; George, S. M. *Surf. Rev. Lett.* **1999**, *6*, 435.
(15) Klaus, J. W.; George, S. M. *Surf. Sci.* **2000**, *447*, 81.
(16) George, S. M.; Ott, A. W.; Klaus, J. W. *J. Phys. Chem.* **1996**, *100*, 13121.
(17) Berland, B. S.; Gartland, I. P.; Ott, A. W. George, S. M. *Chem. Mater.* **1998**, *10*, 3941.
(18) Ehrlich, D. J.; Melngailis, J. *Appl. Phys. Lett.* **1991**, *58*, 2675.

10.1021/cm000313t CCC: $19.00
Published on Web 10/21/2000

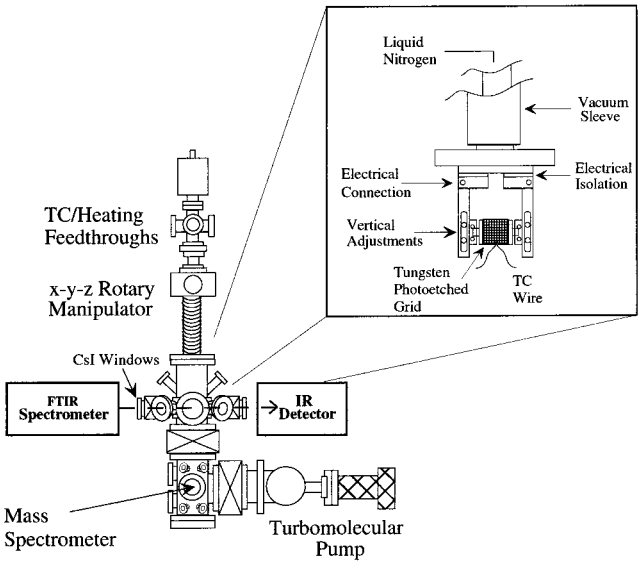

Figure 1. Schematic of the vacuum chamber and sample mount used for transmission FTIR studies of SiO_2 ALD on BN particles.

into two separate $SiCl_4$ and H_2O reactions:[11, 12]

$$\text{(A) } SiOH^* + SiCl_4 \rightarrow SiOSiCl_3^* + HCl \quad (2)$$

$$\text{(B) } SiCl^* + H_2O \rightarrow SiOH^* + HCl \quad (3)$$

where * indicates a surface species. Each of the surface reactions is observed to be self-limiting. Sequential exposure to $SiCl_4$ and H_2O can deposit ~0.9 Å per AB cycle at 700 K or 2.1 Å per AB cycle at room temperature using a Lewis base catalyst such as pyridine or NH_3.[12−15] Atomic force microscope (AFM) images show that the deposited SiO_2 films are very smooth with a roughness nearly identical to the roughness of the initial substrate.[12,13]

In this paper, SiO_2 films are deposited on BN particles using alternating exposures of $SiCl_4$ and H_2O at 700 K. The surface chemistry during the $SiCl_4$ and H_2O exposures is monitored with transmission Fourier transform infrared (FTIR) spectroscopy. Additionally, the FTIR spectra reveal SiO_2 bulk vibrational modes that grow versus the number of AB reaction cycles. The SiO_2 films on the BN particles after 32 AB reaction cycles are then analyzed using transmission electron microscopy (TEM) and X-ray photoelectron spectroscopy (XPS). These FTIR, TEM, and XPS studies all reveal that the SiO_2 films can be grown on the BN particles using sequential surface reactions.

II. Experimental Section

A vacuum apparatus designed for in situ transmission FTIR vibrational spectroscopy studies was used to deposit SiO_2 on the BN particles.[19] FTIR spectroscopy provides an effective way to monitor the surface chemistry occurring during SiO_2 ALD. A schematic of this apparatus is shown in Figure 1. The vacuum apparatus is comprised of two chambers separated by a gate valve. The FTIR studies were conducted in the upper chamber. This chamber is equipped with a Baratron capacitance manometer and several leak valves for controlling the reactant exposures. The lower chamber was maintained at high vacuum by a 200 L s^{-1} turbomolecular pump. This chamber contained an ion gauge and a Dycor quadrupole mass spectrometer.

Samples with a high surface area are necessary for transmission FTIR spectroscopy studies. HCV Grade BN particles from Advanced Ceramics Corp. provided a sufficient surface area for the FTIR studies. These particles are ~10 μm agglomerates composed primarily of ~0.1−0.5 μm turbostratic BN crystals with a total surface area of ~40 m^2/g.[20] Turbostratic and hexagonal BN crystals are both composed of graphitic layers. Turbostratic BN is composed of randomly stacked graphitic layers. In contrast, the graphitic layers of hexagonal BN are ordered with B and N on top of each other in adjacent layers.[21]

A tungsten photoetched grid from Buckbee Mears in St. Paul, MN, was used as a support for the BN particles. This tungsten grid had dimensions of 2 cm × 3 cm, a thickness of 0.002 in., and a grid spacing of 100 lines per inch. Polished stainless steel dies and a manual press were used to press the BN particles into the tungsten grid.[22] A tantalum foil was spot-welded to each side of the tungsten grid to provide electrical contact and facilitate resistive heating. This sample was then suspended between two copper clamps on the sample manipulator as shown in Figure 1. A Chromel−Alumel thermocouple was attached to the center of the tungsten grid using Aremco (Type 571) ceramic adhesive. This thermocouple provided accurate monitoring of the sample temperature.

An $x-y-z$ rotary manipulator equipped with a liquid N_2 cryostat held the sample mount containing the tungsten grid. The $x-y-z$ adjustment capabilities of the manipulator were used to align the BN sample in the infrared beam. The manipulator also contained current and thermocouple feedthroughs for sample heating and temperature regulation. Sample temperatures could be achieved and maintained from 300 to 1100 K without the use of liquid N_2 in the cryostat. The sample was held at 700 K during all of the $SiCl_4$ and H_2O exposures.

For low-pressure exposures, reactant gases were introduced into the upper chamber while the gate valve was open between the upper and lower chambers. The ion gauge was used to measure these reactant pressures ranging from 1×10^{-4} to 1×10^{-3} Torr. A second gate valve between the lower chamber and the turbomolecular pump could be throttled to adjust the pumping speed. The gate valve between the upper and lower chambers was closed for higher reactant pressures. These static pressures ranged from 0.01 to 10 Torr and were measured using the Baratron capacitance manometer.

Following the higher pressure exposures, a liquid N_2 trap backed by a mechanical pump was used to evacuate the upper chamber. The gate valves to the lower chamber and turbomolecular pump were then opened and this further reduced the chamber pressure. This pumping sequence yielded pressures less than 2.0×10^{-6} Torr between $SiCl_4$and H_2O exposures. Pressures this low were needed to minimize the possibility of SiO_2 CVD on the BN particles.

The vibrational spectroscopic data was obtained using a Nicolet Magna 560 Fourier transform infrared (FTIR) spectrometer with an MCT-B infrared detector. The infrared beam passed through two 13 mm thick CsI windows on the upper chamber. Gate valves isolated the CsI windows from the chamber during reactant exposures to prevent deposition on the windows. All of the spectra in this study were recorded at a sample temperature of 350 K after evacuation of the chamber.

Transmission electron microscopy (TEM) and X-ray photoelectron spectroscopy (XPS) data were obtained at the Center for Micro-Engineered Materials at the University of New Mexico by Dr. Paolina Atanassova. An HRTEM JEOL 2010

(19) Dillon, A. C.; Robinson, M. B.; Han, M. Y.; George, S. M. *J. Electrochem. Soc.* **1992**, *139*, 537.

(20) Dowell, M. Advanced Ceramics Corp., Cleveland, OH, personal communication, 1999

(21) Baraton, M. I.; Merle, T.; Quintard, P.; Lorenzelli, V. *Langmuir* **1993**, *9*, 1486.

(22) Ballinger, T. H.; Wong, J. C. S.; Yates, J. T. *Langmuir* **1992**, *8*, 1676.

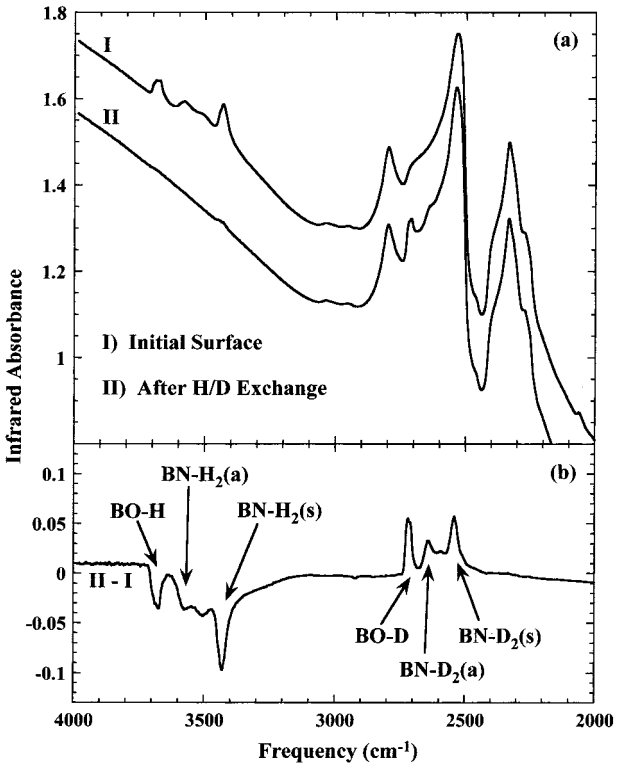

Figure 2. (a) FTIR spectra of the BN particles before (I) and after (II) D_2O exposure at 700 K. (b) FTIR difference spectrum II − I showing the result of H/D exchange.

high-resolution transmission electron microscope was used to obtain the TEM images. These TEM measurements used electron dispersive spectroscopy and a GATAN digital micrograph with a slow scan CCD camera. The TEM analysis monitored the thickness and morphology of the SiO_2 coating on the crystalline BN particles.

An AXIS HSi Kratos Analytical XPS spectrometer was used to obtain the X-ray photoelectron spectra. The XPS chamber had a base pressure of 1×10^{-9} Torr. The XPS data were obtained working in E = constant mode at a pass energy of 80 eV using an Al anode (1486.7 eV energy at 15 kV, 15 mA) in a slot mode. A survey spectrum and high-resolution spectra were obtained for the energy regions of Si 2p, O 1s, B 1s, and N 1s. Depth-profiling studies of the SiO_2 films were obtained by Ar^+ ion sputtering at an estimated etch rate of 1.5 nm/min.

III. Results

Transmission FTIR spectroscopy was used to analyze the initial surface of the BN particles. After the sample was loaded in the chamber, an H_2O adlayer was observed on the BN particles at 300 K. The H_2O adlayer on the BN surface was removed by annealing the sample in vacuum to 700 K. H/D exchange achieved by D_2O exposure at 700 K was then employed to characterize the surface functionality of the annealed BN particles. The FTIR spectra before and after the H/D exchange are shown in Figure 2.

Spectrum I in Figure 2a shows the spectrum of the BN particles before the D_2O exposure. Spectrum II in Figure 2a displays the spectrum after the D_2O exposure. Spectrum II has been displaced for clarity in presentation. Figure 2b shows the difference spectrum II − I. This difference spectrum shows the changes in infrared absorbance that result from H/D exchange. The H/D exchange during the D_2O exposure leads to a decrease in infrared absorbance for hydrogen-containing vibrational features and a concurrent increase in infrared absorbance for deuterium-containing vibrational features.

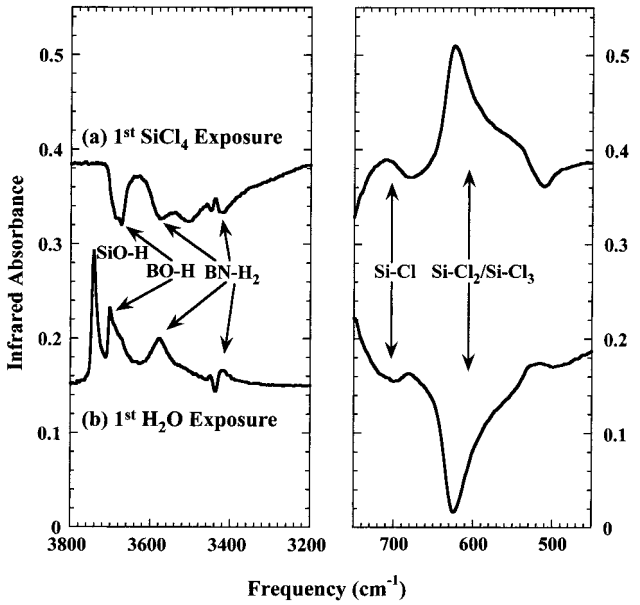

Figure 3. FTIR difference spectra of the BN particles in the O−H, N−H, and Si−Cl stretching regions after (a) the first $SiCl_4$ exposure at 700 K and (b) the first H_2O exposure at 700 K. The reference spectra were recorded prior to the $SiCl_4$ and H_2O exposures.

The initial BN surface functionality is revealed by the negative infrared absorbance features. The negative features correspond to BO−H stretching vibrations at 3677 cm^{-1} and BN−H_2 asymmetric and symmetric stretching vibrations at 3575 and 3430 cm^{-1}, respectively. The new surface vibrational modes resulting from H/D exchange are observed as positive infrared absorbance features. These positive vibrational features are consistent with BO−D stretching vibrations at 2715 cm^{-1} and BN−D_2 asymmetric and symmetric stretching vibrations at 2643 and 2542 cm^{-1}, respectively. The BO−H and BN−H_2 vibrational frequencies and their shifts following H/D exchange are in close agreement with previous studies.[21,23] A BN−H stretching vibration may also coincide with the BN−H_2 symmetric stretching vibration at 3430 cm^{-1}.

SiO_2 was deposited on the BN particles by sequential exposures to $SiCl_4$ and H_2O. The FTIR difference spectra after the first $SiCl_4$ and H_2O exposures are shown in Figure 3. Each spectrum is referenced to the spectrum prior to the exposure. These spectra are displaced from the origin for clarity in presentation. Figure 3a shows the infrared difference spectrum after the first $SiCl_4$ exposure at 700 K. The BO−H stretching vibration at 3680 cm^{-1} and the BN−H_2 stretching vibrations at 3430 and 3575 cm^{-1} are both lost and appear as negative features. The $SiCl_4$ reaction also adds a broad vibrational feature at ~625 cm^{-1} that is assigned to Si−Cl_3 and/or Si−Cl_2 stretching vibrations.[24,25] An additional

(23) Baraton, M. I.; Boulanger, L.; Cauchetier, M.; Lorenzelli, V.; Luce, M.; Merle, T.; Quintard, P.; Zhou, Y. H. *J. Eur. Ceram. Soc.* **1994**, *13*, 371.

(24) Fink, P.; Plotzki, I. *Wiss. Z. Friedrich-Schiller-Univ. Jena, Math.-Naturwiss* **1980**, *29*, 809.

(25) Lang, S. J.; Morrow, B. A. *J. Phys. Chem.* **1994**, *98*, 13314.

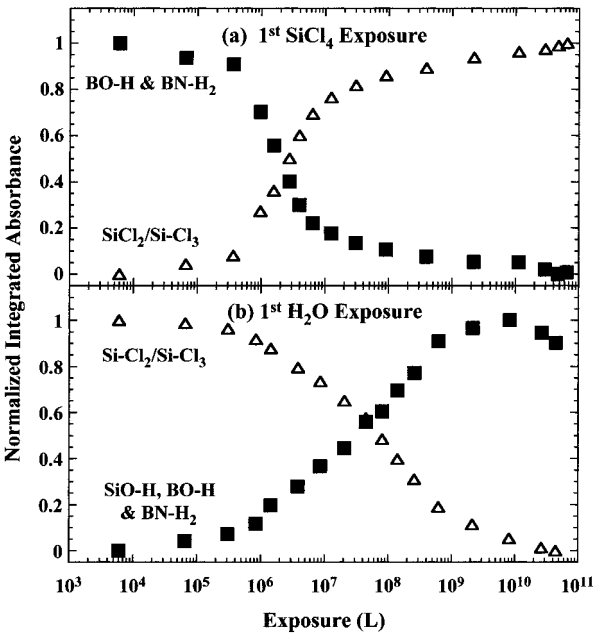

Figure 4. Normalized integrated absorbance of the BO−H and BN−H_2 stretching vibrations and the Si−Cl_2/$SiCl_3$ stretching vibrations versus (a) $SiCl_4$ exposure and (b) H_2O exposure during the first AB cycle at 700 K.

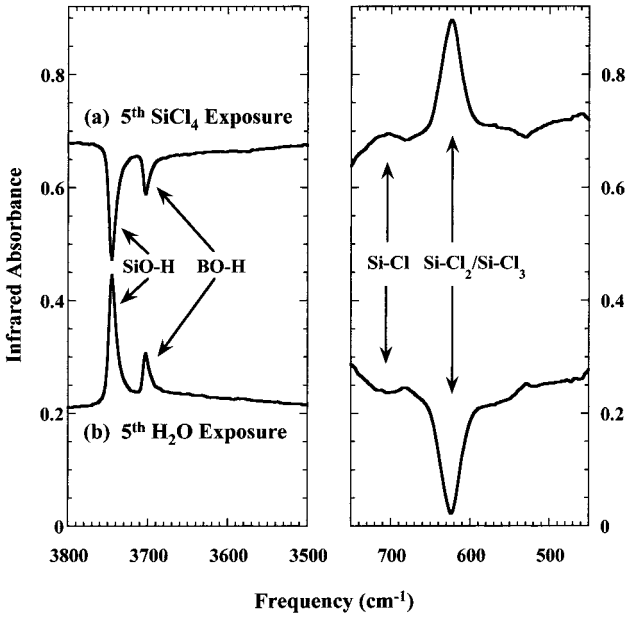

Figure 5. FTIR difference spectra of the BN particles in the O−H and Si−Cl stretching regions after (a) the fifth $SiCl_4$ exposure at 700 K and (b) the fifth H_2O exposure at 700 K. The reference spectra were recorded prior to the $SiCl_4$ and H_2O exposures.

vibrational feature at 710 cm^{-1} is observed and attributed to an Si−Cl stretching vibration.[24,25]

The infrared difference spectrum after the first H_2O exposure at 700 K is shown in Figure 3b. The loss of the Si−Cl_x stretching vibrations indicates that the H_2O exposure removes all of the $SiCl_x$* species that were added during the previous $SiCl_4$ exposure. A new positive infrared absorbance also appears at 3742 cm^{-1}. This new vibrational feature is attributed to an SiO−H stretching vibration and the addition of SiOH* surface species. Accompanying the new SiO−H feature is the reappearance of BO−H and BN−H_2 stretching vibrations that were present on the initial BN surface.

The integrated absorbances for the BO−H, SiO−H, and Si−Cl_2/Si−Cl_3 stretching vibrational features versus $SiCl_4$ and H_2O exposure at 700 K were examined during the first and fifth AB cycles. Figure 4 displays the integrated absorbances during the first $SiCl_4$ and H_2O exposures at 700 K. Figure 4a shows that an $SiCl_4$ exposure of $\sim 1 \times 10^{10}$ L is needed for the first $SiCl_4$ reaction to reach completion. The integrated absorbance versus H_2O exposure displayed in Figure 4b indicates that an H_2O exposure of $\sim 1 \times 10^{10}$ L is also required for the first H_2O reaction to eliminate nearly all of the Si−Cl_2*/Si−Cl_3* species. The slight reduction in the integrated absorbance for the SiO−H, BO−H, and BN−H_2 vibrational features after $>10^{10}$ L H_2O exposures is associated with the conversion of SiOH* surface species to SiO_2. This conversion is observed as a slight decrease in the SiO−H stretching vibration at 3740 cm^{-1} and an increase in the broad absorption band for bulk SiO_2 at $\sim$1100 cm^{-1}.

Figure 5 shows the FTIR difference spectra recorded after the fifth $SiCl_4$ and H_2O exposures at 700 K. The spectra are again displaced for clarity in presentation. Following the $SiCl_4$ exposure, Figure 5a shows that the SiO−H and BO−H stretching vibrations are lost as $SiCl_x$* species are added to the surface. Figure 5b reveals that subsequent H_2O exposure leads to the reappearance of SiO−H and BO−H stretching vibrations and the loss of the Si−Cl_x stretching vibrations. The BOH* species during this fifth AB cycle appear at 3703 cm^{-1}. This vibrational frequency is blue-shifted relative to the frequency of the BOH* species on the initial BN surface at 3677 cm^{-1}.

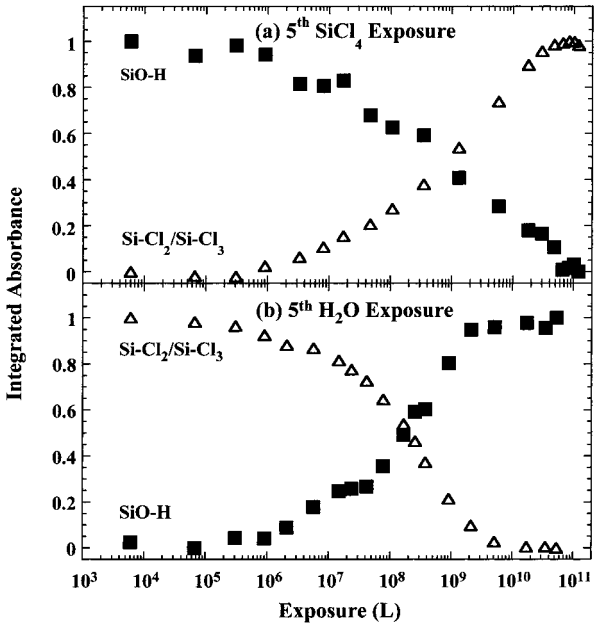

Figure 6. Normalized integrated absorbance of the SiO−H stretching vibration and the Si−Cl_2/$SiCl_3$ stretching vibrations versus (a) $SiCl_4$ exposure and (b) H_2O exposure during the fifth AB cycle at 700 K.

The integrated absorbances for the BO−H, SiO−H, and Si−Cl_2/Si−Cl_3 stretching vibrational features versus $SiCl_4$ and H_2O exposure at 700 K during the fifth AB cycle are shown in Figure 6. The results are similar to the results obtained during the first AB cycle. $SiCl_4$

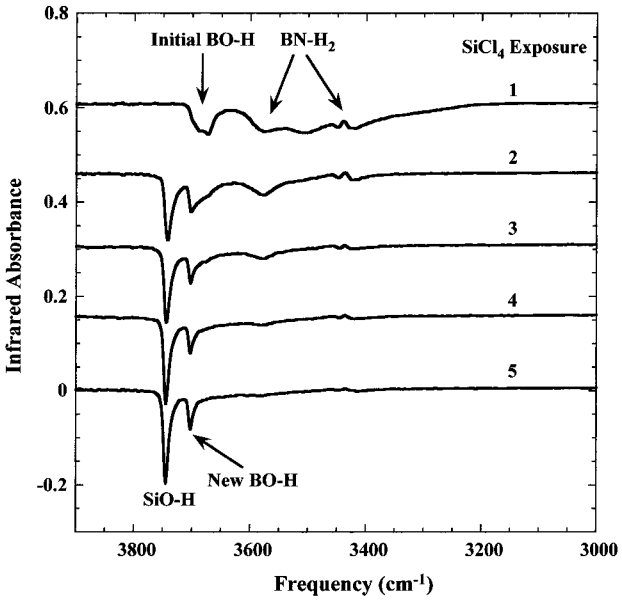

Figure 7. FTIR difference spectra of the BN particles in the O−H and N−H stretching regions after the first five $SiCl_4$ exposures at 700 K. Each spectrum is referenced to the spectrum taken prior to the $SiCl_4$ exposure.

exposures of $\sim 1 \times 10^{10}$ L were needed for completion of the $SiCl_4$ reaction. H_2O exposures of $\sim 1 \times 10^{10}$ L were also sufficient for the H_2O reaction to reach completion. Given these results, SiO_2 films were grown on the BN particles using $SiCl_4$ and H_2O exposures of $\geq 5 \times 10^{10}$ L.

The spectra of the surface hydroxyl species that react with $SiCl_4$ during the first five AB cycles at 700 K are shown in Figure 7. Most of these spectra have been displaced for ease in comparison. The difference spectrum after the first $SiCl_4$ exposure has been referenced to the spectrum of the initial BN surface. The negative absorbance features correspond to the removal of the initial BOH* and BNH_2* species. The remaining difference spectra show the surface hydroxyl species that react with $SiCl_4$ during subsequent $SiCl_4$ exposures. These spectra are all referenced to the spectra recorded prior to the $SiCl_4$ exposures. The spectra show the evolution from BOH* and BNH_2* species on the initial BN surface to SiOH* species and the frequency-shifted BOH* species at 3703 cm^{-1} on the SiO_2-coated BN surface.

The integrated absorbances of the SiO−H, Si−Cl_2/Si−Cl_3, and BO−H vibrational stretching regions were monitored after every $SiCl_4$ and H_2O reactant exposure at 700 K for 32 consecutive AB cycles. Figure 8 shows the integrated absorbances for the SiO−H and Si−Cl_2/Si−Cl_3 stretching vibrations plotted versus AB cycle. The solid circles in Figure 8a show the oscillation of the SiO−H integrated absorbance versus $SiCl_4$ and H_2O exposures at 700 K. The SiO−H integrated absorbance is always lower after the $SiCl_4$ exposure. The difference in integrated absorbance after $SiCl_4$ and H_2O exposures remains fairly constant throughout the 32 AB cycles. The slight rise in the SiO−H integrated absorbance can be attributed to hydroxyl incorporation into the growing SiO_2 film.

The oscillation of the Si−Cl_2/Si−Cl_3 integrated absorbance versus $SiCl_4$ and H_2O exposures at 700 K is

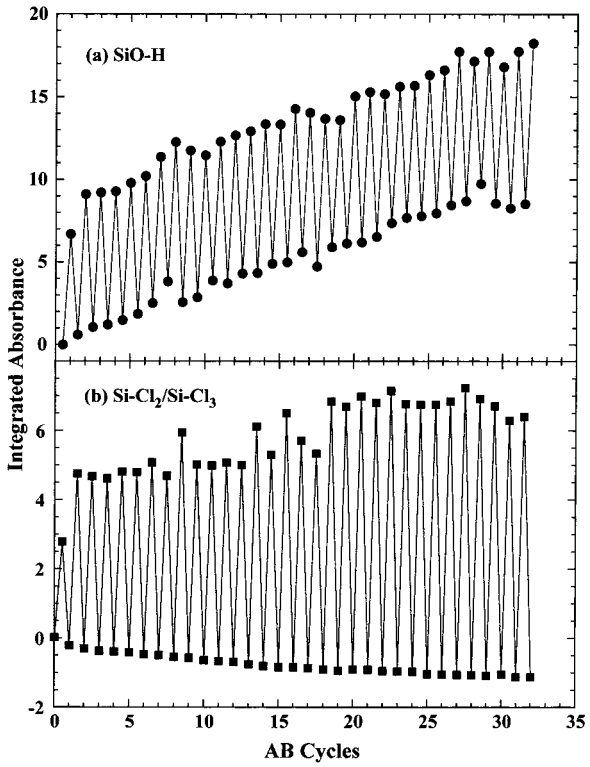

Figure 8. Integrated absorbance of (a) the SiO−H stretching vibrations and (b) the Si−Cl_2/Si−Cl_3 stretching vibrations versus AB cycles at 700 K.

shown by the solid squares in Figure 8b. The Si−Cl_2/Si−Cl_3 integrated absorbance is always lower and approximately equal to zero after the H_2O exposures. The changes in the Si−Cl_2/Si−Cl_3 integrated absorbance are difficult to quantify exactly because of the complications in integrating the Si−Cl_2/Si−Cl_3 stretching region. The Si−Cl_2/Si−Cl_3 stretching vibrations overlap with the bulk SiO_2 vibrational modes that are growing versus AB cycle.

After several AB cycles, a new vibrational feature at 3703 cm^{-1} was added and removed with sequential H_2O and $SiCl_4$ exposures at 700 K, as shown in Figures 5 and 7. This new feature is assigned to BO−H stretching vibrations that are perturbed by the deposition of SiO_2 on the BN particle.[26,27] This BO−H stretching vibration was monitored throughout the 32 AB cycles. The solid triangles in Figure 9 show the integrated absorbance of the BO−H stretching vibration at 3703 cm^{-1} versus AB cycle after the third $SiCl_4$ exposure. The integrated absorbance increases and decreases as BOH* species are alternately added and removed by H_2O and $SiCl_4$ exposures, respectively. The intensity of the BO−H vibrational feature decreases versus AB cycle. The integrated absorbance after 32 AB cycles is only ~30% of the maximum integrated absorbance observed after the fifth H_2O exposure.

The growth of the SiO_2 film on the BN particles was also monitored in the FTIR spectra. The SiO_2 bulk infrared absorption modes appeared at ~450, ~830, and ~1100 cm^{-1}.[28] The increase in the infrared absorbance

(26) Hair, M. L.; Hertl, W. *J. Phys. Chem.* **1973**, *77*, 1965.
(27) Bartram, M. E.; Moffat, H. K. *J. Vac. Sci. Technol. A* **1994**, *12*, 1027.
(28) Nyquist, R. A.; Kagel, R. O., Eds. *Infrared Spectra of Inorganic Compounds;* Academic Press: London, 1997; Vol. IV.

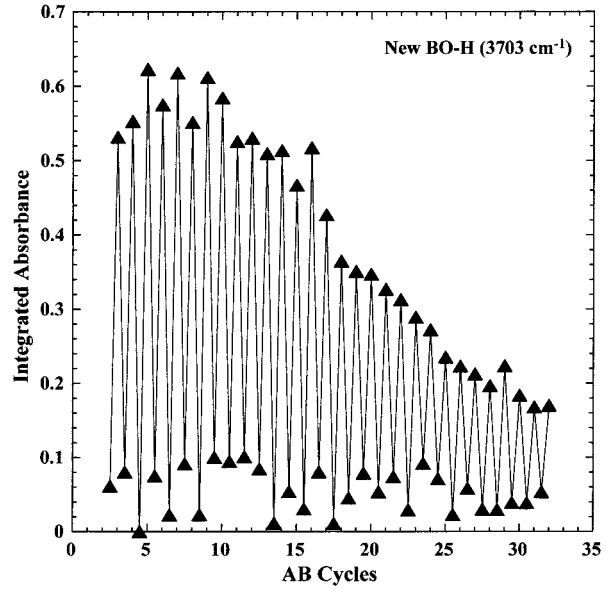

Figure 9. Integrated absorbance of the new BO−H stretching vibration at 3703 cm^{-1} versus AB cycles at 700 K.

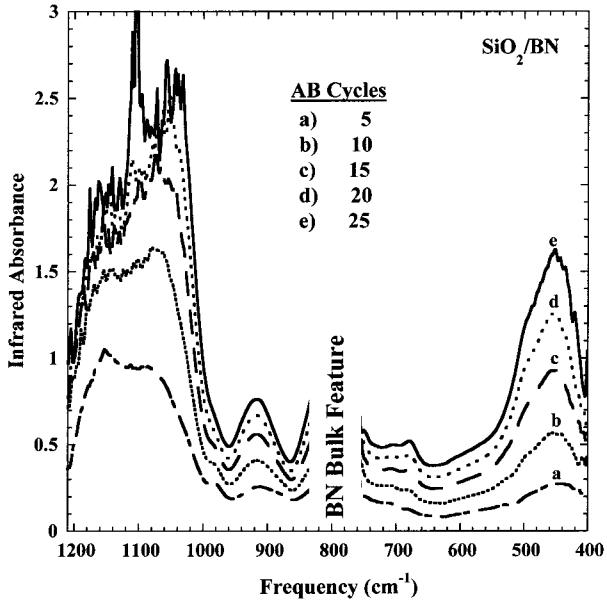

Figure 10. FTIR difference spectra showing the growth of SiO_2 bulk vibrational modes on BN particles versus AB cycles at 700 K. All spectra are referenced to the spectrum of the BN particles before the first AB cycle.

of these vibrational modes versus the number of AB cycles at 700 K is shown in Figure 10. The absorption feature at ∼800 cm^{-1} is associated with a strong BN bulk mode.[29] This absorbance is not easily subtracted in the difference spectra and leads to large fluctuations that have been removed from Figure 10.

The conformality of the SiO_2 coatings on the BN particles was evaluated using transmission electron microscopy (TEM). TEM images of SiO_2-coated BN particles are shown in Figures 11 and 12. These SiO_2 films were grown using 32 $SiCl_4/H_2O$ exposures at 700 K. The TEM image in Figure 10 reveals that the SiO_2 film is deposited on the edge plane of a crystalline BN particle. In contrast, SiO_2 deposition does not occur uniformly on the basal planes. Some areas of the basal plane are coated with SiO_2 and other areas are void of SiO_2 deposition. Figure 11 shows a TEM image of another BN particle that illustrates the nonuniform deposition on the basal plane after 32 AB cycles.

X-ray photoelectron spectroscopy (XPS) measurements were also performed on the SiO_2-coated BN particles. An XPS spectrum for uncoated BN particles observed photoelectrons corresponding to binding energies at 190 eV (B 1s) and 397 eV (N 1s). An XPS measurement on the BN particles after 32 $SiCl_4/H_2O$ exposures observed that the intensities of the B and N photoelectrons were only partially diminished after 32 $SiCl_4/H_2O$ exposures. Photoelectrons were also monitored corresponding to binding energies at 103 eV (Si 2p) and 532 eV (O 1s). These results suggest that there are open areas on the BN surface or areas covered with only a very thin SiO_2 film. These XPS results are consistent with the TEM images.

IV. Discussion

SiO_2 atomic layer deposition (ALD) has been studied in several previous investigations.[11−15] FTIR studies showed that the $SiCl_4$ and H_2O half-reactions were self-limiting and went to completion at 600 K.[11] SiO_2 ALD growth rates on an Si(100) substrate were measured using ellipsometric studies.[12] Deposition rates of 1.1 Å/AB cycle, 0.87 Å/AB cycle, and 0.75 Å/AB cycle were measured at 600, 700, and 800 K, respectively.[12] In addition, the sequential surface reactions used for SiO_2 ALD can be catalyzed using Lewis bases such as pyridine and ammonia.[13−15] These Lewis bases can reduce the temperature for SiO_2 ALD growth to room temperature.[13−15]

The ABAB... reaction cycles for SiO_2 ALD were initiated using the BOH* and BNH_2* species on the initial BN surface. In previous studies, SiO_2 ALD was initiated by reacting $SiCl_4$ with SiOH* species on a starting SiO_2 film on Si(100)[12] or porous silicon substrate.[11] Figure 2 demonstrates the existence of BOH* and BNH_2* species on the initial BN surface. Figure 3a shows that $SiCl_4$ reacts with both the BOH* and BNH_2* species at 700 K and yields new $SiCl_x$* species. Figure 3b reveals that the subsequent H_2O exposure at 700 K removes the $SiCl_x$* species and adds a new SiOH* species. The subsequent switching between SiOH* and $SiCl_x$* species is observed after each sequential H_2O and $SiCl_4$ exposure.

Figure 7 shows the surface species that react with $SiCl_4$ at 700 K during the first five AB cycles. BO−H and BN−H_2 stretching vibrational features are clearly observed as negative infrared absorbance features after the first $SiCl_4$ exposure. These negative absorbance features decrease progressively during the second, third, and fourth $SiCl_4$ exposures. The initial BO−H and BN−H_2 stretching vibrational features observed on the initial BN surface were not monitored after the fifth and all subsequent $SiCl_4$ exposures. The disappearance of these vibrational features argues that SiO_2 growth has occurred on the portion of the BN surface that originally produced these vibrational features.

Figures 3 and 7 reveal that an SiO−H vibrational stretch appears during the first AB cycle after the H_2O

(29) Geick, R.; Perry, C. H.; Rupprecht, G. *Phys. Rev.* **1966**, *146*, 543.

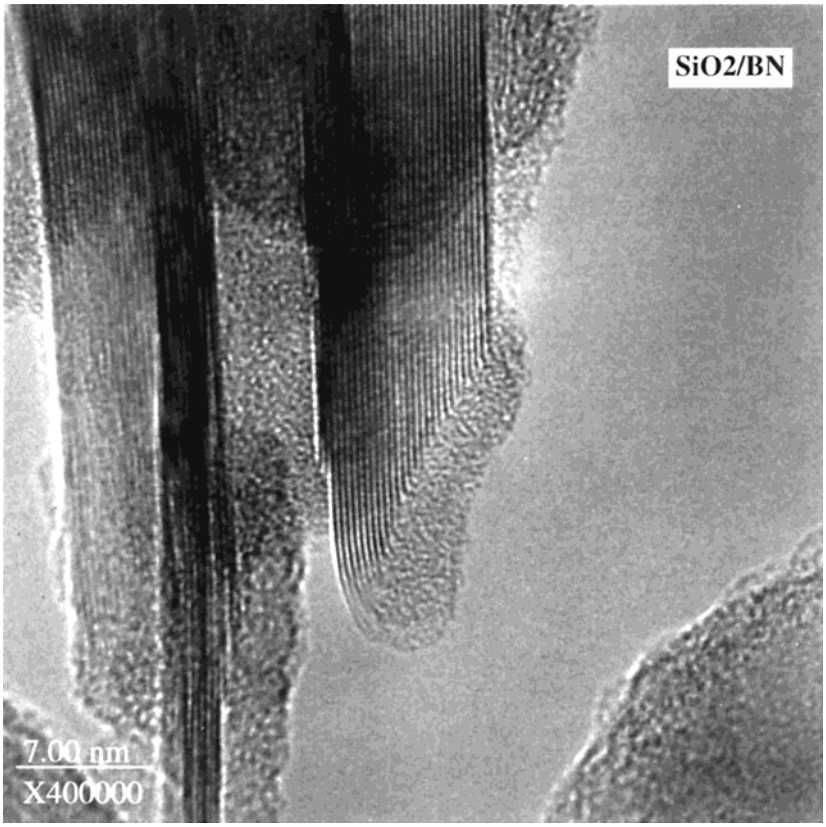

Figure 11. Transmission electron microscope image of a BN particle after 32 $SiCl_4/H_2O$ reaction cycles at 700 K. The edge plane of the BN particle is coated with an SiO_2 film with a thickness of ~28−38 Å.

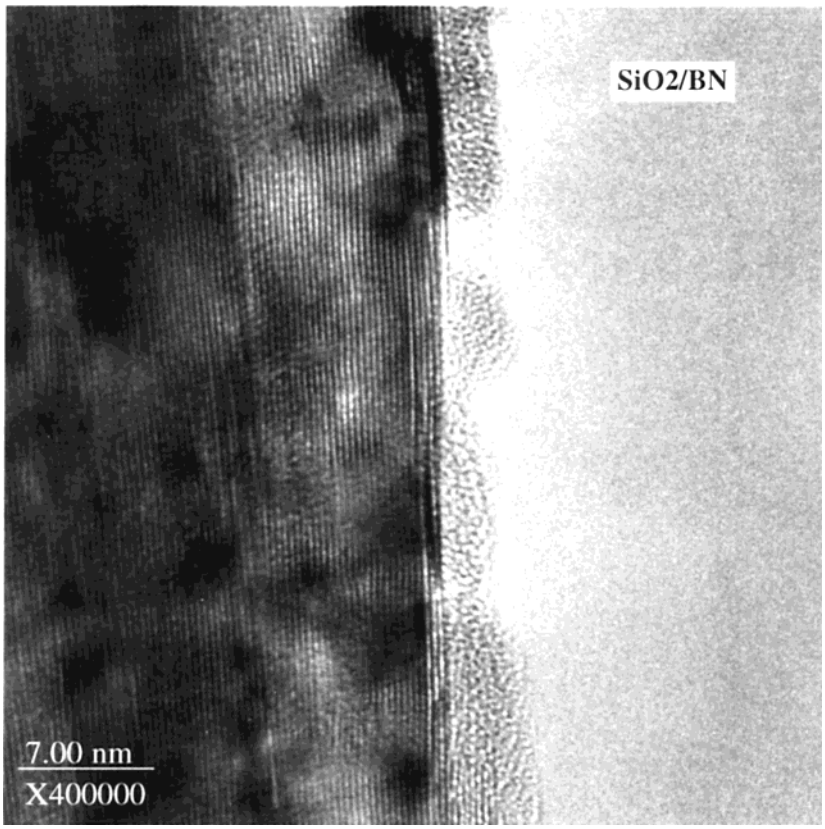

Figure 12. Transmission electron microscope image of the basal plane of a BN particle after 32 $SiCl_4/H_2O$ reaction cycles at 700 K.

exposure at 700 K. The progressive increase in the integrated absorbance for the SiO−H stretching vibration versus AB cycles shown in Figure 8a suggests that hydroxyls are becoming incorporated into the SiO_2 film. Similar hydroxyl incorporation was observed during Al_2O_3 ALD using $Al(CH_3)_3$ and H_2O sequential expo-

sures at 450 K.[30] The hydroxyl incorporation after 32 AB cycles is equivalent to approximately one monolayer of SiOH* species. On the basis of previous results for hydroxyl incorporation during Al_2O_3 ALD,[30] this hydroxyl concentration in the SiO_2 film is expected to be removed by annealing the SiO_2-coated BN particles to ~1000 K.

A new infrared absorption peak at 3703 cm^{-1} is also observed in Figures 3 and 7 after the first H_2O exposure at 700 K. This vibrational feature can be assigned to a new BOH* species. An identical mode at 3703 cm^{-1} is ascribed to a BO−H vibration following BCl_3 adsorption and subsequent hydrolysis on silica surfaces.[26] An equivalent vibrational frequency of 3703 cm^{-1} is also monitored after $B(OCH_3)_3$ adsorption and subsequent hydrolysis on silica surfaces.[27]

Figures 3 and 9 show that the new BO−H vibrational feature at 3703 cm^{-1} grows quickly and then slowly decreases during the 32 AB cycles at 700 K. The existence of this BO−H vibrational feature suggests that portions of the BN surface are not initially reactive toward $SiCl_4$ or H_2O. The new BOH* species may be adjacent to the deposited SiO_2 on unreactive BN surface area during the 32 AB cycles. There may be a progressive reduction of these unreactive areas during the 32 AB cycles. Another possible explanation for these new BOH* species is B diffusion onto the SiO_2 coating on the BN particle. The identical vibration frequency of 3703 cm^{-1} [26,27] after boron deposition on SiO_2 particles using BCl_3 or $B(OCH_3)_3$ followed by hydroxylation suggests that the boron may be on the deposited SiO_2.

The growth of SiO_2 bulk vibrational modes shown in Figure 10 demonstrates the deposition of SiO_2 on the BN particles. The TEM image in Figure 11 reveals that the edge plane of the BN particle has a fairly uniform SiO_2 coating with a thickness of ~28−38 Å after 32 AB cycles. This thickness is consistent with an SiO_2 deposition rate of ~0.88−1.19 Å/AB cycle at 700 K. This growth rate is in good agreement with the SiO_2 deposition rate of ~0.9 Å/AB cycle at 700 K measured on Si(100) wafers.[12]

The TEM images also reveal that the SiO_2 coating is not as uniform as expected for ideal atomic layer deposition. Figures 11 and 12 show that the basal planes of the BN particles are coated fairly randomly. Some of the basal plane areas are covered with an SiO_2 film that is comparable with the SiO_2 films deposited on the edge planes. Other areas of the basal planes contain less or no SiO_2 deposition.

The edge planes of hexagonal BN will expose dangling bonds on sp^2-hybridized B and N surface atoms. These edge plane surface atoms are expected to react easily with H_2O to yield BOH* and BNH*/BNH_2* species. Previous investigations of $SiCl_4$ reactivity with SiOH* species during SiO_2 ALD suggest that BOH* species should react with $SiCl_4$.[11,12] Earlier studies of $SiCl_4$ reactivity with SiNH* species during Si_3N_4 ALD also suggest that BNH*/BNH_2* species should react with $SiCl_4$.[31] Consequently, the initial reactivity of $SiCl_4$ with the BOH* and BNH*/BNH_2* species on the edge planes of hexagonal BN particles is anticipated and confirmed by the FTIR results shown in Figures 3 and 7.

The basal plane of hexagonal BN particles contains sp^2-hybridized B and N atoms that are fairly chemically inert. Calculations of the electronic structure of the basal plane of hexagonal BN reveal that the B sites are Lewis acid sites and the N sites are Lewis base sites.[32] $SiCl_4$ is not expected to interact with either the Lewis acid or Lewis base sites. H_2O may interact weakly with these sites because of its ability to act as both a weak acid and a weak base. Consequently, SiO_2 ALD on the basal plane of BN may be very difficult without the presence of BOH* or BNH*/BNH_2* species.

The TEM images reveal that SiO_2 films are deposited fairly uniformly on the edge planes of the BN particles. This observation is consistent with the expectation that these edge planes are covered with BOH* and BNH*/BNH_2* species. In contrast, SiO_2 is not deposited uniformly on the basal planes of the BN particles. The SiO_2 is often in patches or entirely absent from regions of the basal plane. The lack of SiO_2 deposition is predicted by the inertness of the basal plane. The presence of patches of SiO_2 is perhaps explained by SiO_2 deposition that may nucleate at step edges on the basal plane. These step edges may contain BOH* and BNH*/BNH_2* species that can react with $SiCl_4$. Many of the TEM images tend to show SiO_2 deposits on the basal plane that appear to originate from a step edge.

The results for SiO_2 deposition on BN particles are different than the results for Al_2O_3 deposition on BN particles.[33] Al_2O_3 ALD on BN particles led to the deposition of uniform and conformal Al_2O_3 coatings.[33] This difference is believed to be related to the difference between the reactants for SiO_2 and Al_2O_3 ALD. The Al atom in the $Al(CH_3)_3$ reactant employed for Al_2O_3 ALD has six electrons in its outer electronic shell. As a result, $Al(CH_3)_3$ is a Lewis acid and can readily accept an electron pair. Because the N atoms on the basal plane of the BN particles have a lone electron pair,[32] $Al(CH_3)_3$ may accept an electron pair from the N atoms and form a N−$Al(CH_3)_3$* species. This N−$Al(CH_3)_3$* species may subsequently react with H_2O and initiate Al_2O_3 deposition on the basal plane.

In contrast to $Al(CH_3)_3$, the Si atom in the $SiCl_4$ reactant has eight electrons in its outer electronic shell and will not display Lewis acid or Lewis base interactions with the basal plane of the BN particles. The $SiCl_4$ may be confined to react only with the BOH* and BNH*/BNH_2* species on the edge planes and the step edges on the basal planes of the BN particles. This limited surface reactivity would predict unreacted BN surface area and explain the observation of BOH* species throughout the 32 AB cycles. The reactivity of $SiCl_4$ with only BOH* and BNH*/BNH_2* surface species is in agreement with the TEM images that show uneven SiO_2 deposition on the basal plane of the BN particles. This specific reactivity of $SiCl_4$ also agrees with the XPS measurements that observe B and N XPS signals that are not completely extinguished by the SiO_2 deposition.

The SiO_2 films deposited with atomic layer control using alternating $SiCl_4$ and H_2O exposures at 700 K are

(30) Dillon, A. C.; Ott, A. W.; Way, J. D.; George, S. M. *Surf. Sci.* **1995**, *322*, 230.
(31) Klaus, J. W.; Ott, A. W.; Dillon, A. C.; George, S. M. *Surf. Sci.* **1998**, *418*, L14.
(32) Yamamura, S.; Takata, M.; Sakata, M. *J. Phys. Chem. Solids* **1997**, *58*, 177.
(33) Ferguson, J. D.; Weimer, A. W.; George, S. M. *Thin Solid Films* **2000**, *371*, 95.

not completely uniform and conformal on the BN particles. However, these ultrathin SiO_2 films should still be useful to increase the loading of BN particles in composite materials for thermal management applications. The patches of SiO_2 deposited on the edge planes and portions of the basal planes should facilitate the coupling of the BN particles to the epoxy matrix of composite materials. The deposition of SiO_2 only on the edge planes may also prove to be advantageous. Low SiO_2 deposition on the basal planes may promote the stacking of BN platelets with parallel *c*-axes. This stacking geometry may be desirable for high thermal conductivity in BN composites.

V. Conclusions

SiO_2 was deposited with atomic layer control on BN particles using sequential surface reactions. Sequential exposures to $SiCl_4$ and H_2O at 700 K deposited silicon and oxygen as the surface was alternately covered by $SiCl_x$* and SiOH* species. FTIR spectroscopic studies monitored the surface species and bulk SiO_2 vibrational modes during the $SiCl_4$ and H_2O exposures. The FTIR spectra observed a new BOH* vibrational feature at 3703 cm^{-1} that suggested that the SiO_2 deposition did not completely cover the BN particle. The TEM images revealed SiO_2 deposition on the edge planes and only uneven deposition on the basal planes of the BN particles. The XPS analysis was also consistent with nonconformal SiO_2 deposition. This uneven SiO_2 deposition is consistent with $SiCl_4$ reacting only on the initial BOH* and BNH*/BNH_2* species on the edge planes or defects on the basal plane of the BN particles. The SiO_2 deposition on BN particles should be useful to increase the loading of BN particles in composite materials.

Acknowledgment. This work was supported by the Center for Micro-Engineered Materials (CMEM) at the University of New Mexico (UNM). The authors thank Dr. Paolina Atanassova (CMEM/UNM) for performing the TEM and XPS analysis. The authors also thank Advanced Ceramics Corp. for providing the BN particles. The Nicolet Magna 560 FTIR spectrometer was obtained with support from DARPA, in conjunction with the U.S. Army Research Office, under contract number DAAG55-98-C-0036.

CM000313T